

2008

An Object Oriented Program for the Numerical Simulation of Hermetic Reciprocating Compressor Behaviour

Rashmin Damle

Technical University of Catalonia

Joaquim Rigola

Technical University of Catalonia

Carlos D. Perez-Segarra

Technical University of Catalonia

Assensi Oliva

Technical University of Catalonia

Follow this and additional works at: <https://docs.lib.purdue.edu/icec>

Damle, Rashmin; Rigola, Joaquim; Perez-Segarra, Carlos D.; and Oliva, Assensi, "An Object Oriented Program for the Numerical Simulation of Hermetic Reciprocating Compressor Behaviour" (2008). *International Compressor Engineering Conference*. Paper 1911. <https://docs.lib.purdue.edu/icec/1911>

This document has been made available through Purdue e-Pubs, a service of the Purdue University Libraries. Please contact epubs@purdue.edu for additional information.

Complete proceedings may be acquired in print and on CD-ROM directly from the Ray W. Herrick Laboratories at <https://engineering.purdue.edu/Herrick/Events/orderlit.html>

An Object Oriented Program for the Numerical Simulation of Hermetic Reciprocating Compressor Behaviour

Rashmin DAMLE, Joaquim RIGOLA, Carlos D. PÉREZ-SEGARRA, Assensi OLIVA

Centre Tecnològic de Transferència de Calor (CTTC)
 Universitat Politècnica de Catalunya (UPC)
 ETSEIAT, C. Colom 11, 08222 Terrassa (Barcelona), Spain
 Tel. +34-93-739.81.92, Fax: +34-93-739.89.20
 cttc@cttc.upc.edu, <http://www.cttc.upc.edu>

ABSTRACT

An object oriented approach for the numerical simulation of the thermal and fluid dynamic behaviour of hermetic reciprocating compressors is presented in this paper. The compressor domain is formed by connecting individual elements such as tubes, chambers, compression chambers, valve plates, etc., which exchange information (pressure, temperature, mass flow etc.) between themselves. The coupled system is solved until convergence is reached. Code verification tests and numerical results of some illustrative cases are presented to show the possibilities offered by the new program.

1. INTRODUCTION

A numerical simulation model for the thermal and fluid dynamic behaviour of hermetic reciprocating compressors for the analysis of standard domestic/commercial applications has been extensively presented during several Purdue conferences (Pérez-Segarra, et al.,1994), (Escanes, et al.,1996), (Rigola et al.,1998) and published in detail by (Pérez-Segarra, et al.,2003). These studies were focussed on the improvement of the compressor design, reduction of power consumption, increasing the compressor efficiency and optimising the compressor behaviour. The numerical verification and detailed experimental validation have also been shown in depth by (Pérez-Segarra, et al.,2003), (Rigola et al.,2003), (Rigola et al.,2004). The numerical model analysed the fluid flow based on full integration of the one-dimensional transient governing equations (continuity, momentum and energy) through all the compressor domain in a sequential way.

The use of new refrigerants, new compressor circuitry, new designs, some aspects like more than two parallel lines, the possibility to work with more than one compression chamber etc., have obliged to develop new modelling strategies. The thermal and fluid behaviour resolution allowing such flexibility is presented in this article. The numerical simulation consists of components (tubes, chambers, compression chamber, valve orifices, fixed values), which are interlinked exchanging boundary information from each other. The coupled system is solved until the convergence is reached.

2. MODULAR COMPRESSOR DOMAIN

The compressor domain is divided into separate elements (objects from the C++ point of view) as shown in Figure 1. The following objects are programmed:

- “ Tube ”: a tube transporting the gas.
- “ Compression chamber ”: a compression chamber.
- “ Chamber ”: a chamber as a reservoir.
- “ Valve Orifice ”: a valve orifice for valve dynamics.
- “ FixedValue ”: a boundary condition object, at fixed pressure and temperature.

These objects are linked together to form the compressor domain. Each object is capable of solving itself for given boundary conditions.

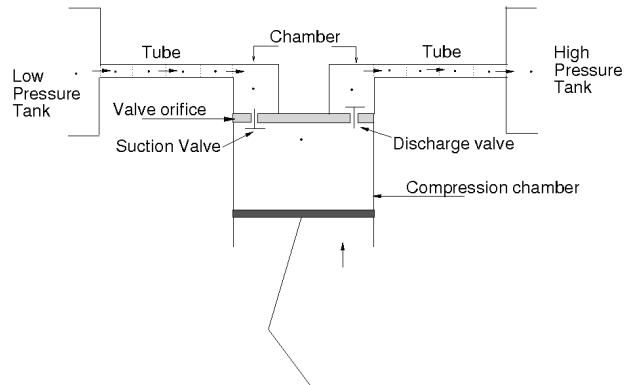


Figure 1: One piston compressor domain formed by different elements (objects)

3. DISCRETIZED EQUATIONS

Each element of the compressor domain is divided into finite control volumes (CVs). For any CV in which the gas is flowing the governing equations (continuity, momentum and energy) can be written in terms of local averaged fluid variables, neglecting body forces, axial shear stresses and axial heat conduction in the following form:

$$\frac{\partial m}{\partial t} + \sum \dot{m}_e - \sum \dot{m}_w = 0 \quad (1)$$

$$\frac{\partial m\bar{v}}{\partial t} + \sum \dot{m}_e v_e - \sum \dot{m}_w v_w = F_s \quad (2)$$

$$\frac{\partial m(\bar{h} + \bar{e}_c)}{\partial t} + \sum \dot{m}_w (h_w + e_{cw}) - \sum \dot{m}_e (h_e + e_{ce}) = V \frac{\partial \bar{p}}{\partial t} + \dot{Q}_{wall} \quad (3)$$

4. NUMERICAL RESOLUTION OF THE COMPRESSOR DOMAIN ELEMENTS

4.1 Tube

A tube as shown in the Figure 2a is solved according to the SIMPLEC algorithm (Patankar, 1980) using staggered arrangement for velocities. Upwind criteria is used for the convective terms. Inlet and outlet

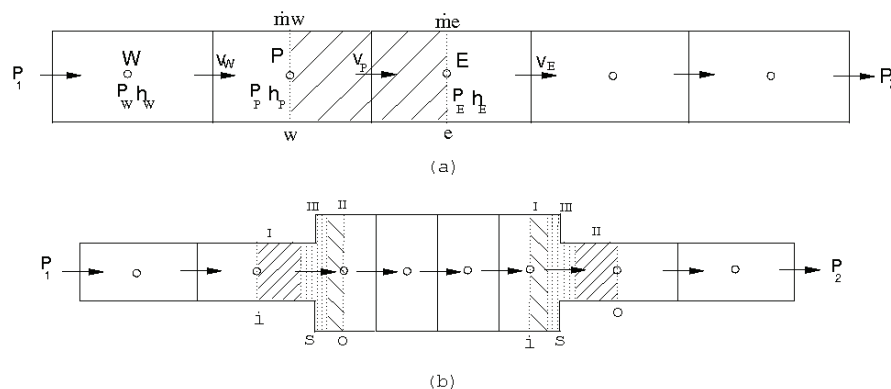


Figure 2: (a) Tube with staggered control volumes, (b) Tube with expansion/contraction

pressures are linked to the tube boundary pressure (p_b) assuming $p_{inlet/outlet} = p_b \pm \frac{\rho v_P^2}{2}$. In case of a sudden

expansion or contraction as shown in Figure 2b, when tubes are connected to other tubes or to chambers, the following relation is used to relate the pressures across the expansion/contraction (Morse, 1953).

$$l \frac{\partial \dot{m}}{\partial t} + \frac{|\dot{m}|v_P}{2} \left(\frac{(S^S)^2}{(S^{II})^2} - \frac{(S^S)^2}{(S^I)^2} \right) + \left(\frac{S^S}{S^o} - \frac{1}{c_c} \right)^2 = (p_i - p_o)S_S \quad (4)$$

The tube gives pressure and mass flow rate as output to the chamber/compression chamber which is used for the first pass through the chamber/compression chamber iterative loop at every iteration.

4.2 Compression Chamber/Chamber

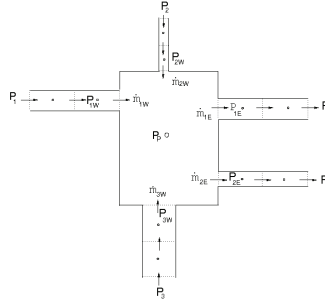


Figure 3: Chamber with multiple inlets and outlets.

Pressure correction approach for the compressor chamber is described in the section. The chamber treatment is similar to that of compression chamber with the volume at the current time step V , equal to that at the previous instant V^0 as the volume of chamber remains constant. The mass flow rate equation for the inlets/outlets of the compression chamber/chamber is written as :

$$\dot{m}_k = \frac{N_k(p_P - p_k) + H_k + \left(\frac{l_k \dot{m}_k^0}{\Delta t} \right)}{M_k} \quad (5)$$

where, the variables take different values for valve orifices and tubes. The subscript k indicates the different elements connected to the compression chamber/chamber. From this equation a mass correction is sought as: $\dot{m}'_k = d_k(p'_P - p'_k)$ where, $d_k = \frac{N_k}{M_k}$ and put in the continuity equation (1) to obtain an equation for pressure correction (p') for compression chamber/chamber. Here, flow entering the chamber is considered positive (west) and leaving as negative (east). The compression chamber/chamber gets pressure from the tubes and valve orifices as data. Thus, $p'_{kE} = 0$ and $p'_{kW} = 0$. The compression chamber/chamber resolution consists of the following steps for every iteration.

1. Guess initial p_P^*, h_P^* and \dot{m}_k^{**} (use the mass flow rate coming from tubes or valve orifices)
2. Calculate the density $\rho_P^* = \rho(p_P^*, h_P^*)$
3. Calculate N_k, H_k, M_k for the respective neighbours (tubes or valve orifices) and calculate new \dot{m}_k^*
4. Calculate p'_P
5. Update: $p_P = p_P^* + \alpha_r p'_P$, $\rho_P = \rho_P^* + \rho'_P$
6. Solve the energy equation and get new value of h_P
7. If *mass residual* > set precision, go to point 2 with $p_P^* = p_P$, $h_P^* = h_P$ and $\dot{m}_k^{**} = \dot{m}_k^*$

4.3 Valve Orifice

The valve orifice object is connected between a chamber and a compression chamber as shown in Figure 4. An equation similar to the expansion/contraction extended to compressible flow used to evaluate mass flow (Browler, 1993), through the valves is:

$$l \frac{\partial \dot{m}}{\partial t} + \frac{|\dot{m}|v_P}{2} \frac{\gamma - 1}{\gamma} \frac{1 - p_o/p_i}{\Pi^{1/\gamma} - \Pi} = (p_i - p_o)KS_s \quad (6)$$

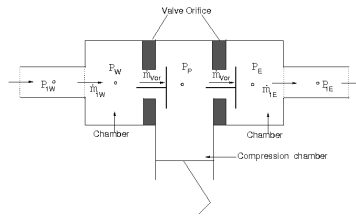


Figure 4: Valve orifice connected between chamber and compression chamber.

It receives pressures (p_i and p_o) on either side of it which are p_W and p_P for the suction side and p_P and p_E on the discharge side as shown in Figure 4. The effective area, KS_s , is then calculated and in turn the mass flow rate. It passes pressures across it and the mass flow rate to its neighbours which is used for the first pass through the chamber/compression chamber iterative loop at every iteration.

4.4 FixedValue

A FixedValue object serves as a boundary condition (fixed pressure and temperature). It only gives the pressure and temperature values as output to the tubes connected to it.

5. GLOBAL ALGORITHM OF RESOLUTION

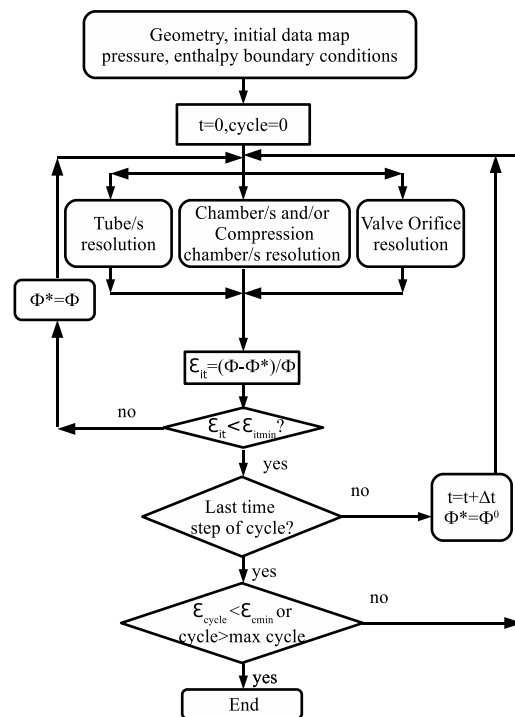


Figure 5: Global algorithm for the simulation of the compressor domain

The global iterative algorithm is shown in the Figure 5. The program control goes through all the elements once every iteration. An iteration for the given element at each time step consists of the following steps:

1. Get inputs (p , h , \dot{m} etc.) from neighbour elements.

2. Solve the governing equations of the element.
3. Set outputs (p, h, \dot{m} etc.) for neighbour elements.

The iterations are continued till the maximum number of iterations or the convergence criteria for each time step is reached. Transient calculation then continues till steady or cyclic steady state is reached.

6. TEST CASES FOR CODE VERIFICATION

6.1 One tube vs. two and three tubes

Mass flow rate at steady state for a tube shown in the Figure 2a is shown in the Table 1. Results for the same tube solved as two/three different tube objects connected to form a single tube with same geometry (20 CVs and a precision of $1e^{-6}$) give mass flow rates of $1.490874e^{-1}$ kg/s and $1.490874e^{-1}$ kg/s respectively.

Table 1: Steady state mass flow rate (kg/s) for tube with $p_{inlet}=55$ bars and $p_{outlet}=50$ bars: evolution with number of nodes (n) and precision (ϵ).

n/ϵ_{steady}	$1e^{-3}$	$1e^{-4}$	$1e^{-5}$	$1e^{-6}$	$1e^{-7}$
5	$1.491375e^{-1}$	$1.490917e^{-1}$	$1.490877e^{-1}$	$1.490873e^{-1}$	$1.490873e^{-1}$
10	$1.491362e^{-1}$	$1.490879e^{-1}$	$1.490874e^{-1}$	$1.490874e^{-1}$	$1.490874e^{-1}$
20	$1.491149e^{-1}$	$1.490890e^{-1}$	$1.490876e^{-1}$	$1.490875e^{-1}$	$1.490875e^{-1}$
40	$1.490832e^{-1}$	$1.490886e^{-1}$	$1.490876e^{-1}$	$1.490875e^{-1}$	$1.490875e^{-1}$
80	$1.491006e^{-1}$	$1.490888e^{-1}$	$1.490876e^{-1}$	$1.490875e^{-1}$	$1.490875e^{-1}$

6.2 Tube-Chamber-Tube / Chamber with multiple inlets and outlets

Results for a chamber connected with two tubes across a pressure difference are shown in the Table 2 while Table 3 shows results for a chamber with multiple tubes of different diameters across a pressure difference as in Figure 3. The sum of the mass flow rates entering and leaving tends to zero at steady state.

Table 2: Steady state mass flow rate (kg/s) for tube-chamber-tube with $p_{inlet}=55$ bars and $p_{outlet}=50$ bars: evolution with number of nodes (n) and precision (ϵ).

n/ϵ_{steady}	$1e^{-4}$	$1e^{-5}$	$1e^{-6}$	$1e^{-7}$	$1e^{-8}$
5	$1.210229e^{-1}$	$1.201000e^{-1}$	$1.209984e^{-1}$	$1.209981e^{-1}$	$1.209982e^{-1}$
10	$1.210213e^{-1}$	$1.209991e^{-1}$	$1.209968e^{-1}$	$1.209965e^{-1}$	$1.209965e^{-1}$
20	$1.210205e^{-1}$	$1.209982e^{-1}$	$1.209960e^{-1}$	$1.209957e^{-1}$	$1.209957e^{-1}$
40	$1.210200e^{-1}$	$1.209978e^{-1}$	$1.209955e^{-1}$	$1.209953e^{-1}$	$1.209953e^{-1}$
80	$1.210199e^{-1}$	$1.209976e^{-1}$	$1.209953e^{-1}$	$1.209951e^{-1}$	$1.209951e^{-1}$

Table 3: Chamber with 3 tube inlets (with diameters d, 0.2d, 0.6d) and 2 outlets (with diameters d, 0.4d, 0.8d) inlet $p_r=55$ bars, outlet $p_r=50$ bars

n/ϵ_{steady}	$1e^{-4}$	$1e^{-5}$	$1e^{-6}$	$1e^{-7}$	$1e^{-8}$
mass residue	$7.621802e^{-4}$	$7.818611e^{-5}$	$7.769957e^{-6}$	$7.715786e^{-7}$	$7.643355e^{-8}$
$\sum \dot{m}_{in}$	$4.370016e^{-1}$	$4.373891e^{-1}$	$4.374283e^{-1}$	$4.374322e^{-1}$	$4.374327e^{-1}$
$\sum \dot{m}_{out}$	$4.377638e^{-1}$	$4.374673e^{-1}$	$4.374361e^{-1}$	$4.374330e^{-1}$	$4.374327e^{-1}$
time(secs)	14.75	16.63	17.25	19.23	20.74

6.3 One piston compressor domain

A single compressor domain without reed valves (valves kept open) is put to equal end pressures in order to check the cyclic operation of the code. As the end pressures are same the sum of mass flow entering and leaving the compression chamber through suction and discharge ports during a cycle should be zero. The value obtained at cyclic state is $0.59e^{-6}$ kg, which is acceptable and verifies the working of the elements put together as compressor domain. Results for one piston compressor domain as in the Figure 1 operating between 30 bars and 80 bars are shown in Table 4. The compressor capacity is 2.65 cm^3 with carbon dioxide as the working fluid.

Table 4: Cyclic state parameters for 1 piston assembly working between 30 bars and 80 bars.

$\epsilon_{\Delta t}/\epsilon_{cyclic}$	$\dot{m}_{[kg/hr]}$	$T_{out}^{\circ C}$	$W(J)$	$avg.iter/cycle$	time(s)
$1e^{-2}$	29.5939	103.9669	-10.1402	8	265
$1e^{-3}$	29.6028	103.9636	-10.1431	11	337
$1e^{-4}$	29.6027	103.9653	-10.1431	19	473
$1e^{-5}$	29.6026	103.9656	-10.1431	23	663
$1e^{-6}$	29.6026	103.9656	-10.1431	38	963
$1e^{-7}$	29.6026	103.9656	-10.1431	55	1357

7. ILLUSTRATIVE CASES

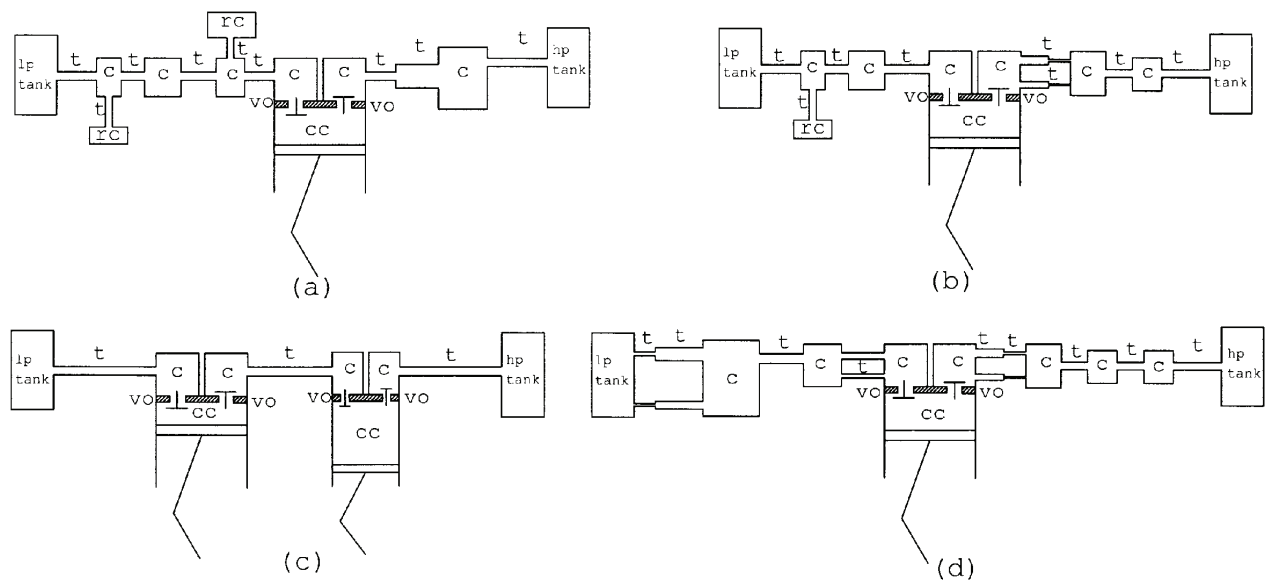


Figure 6: Different compressor configurations (lp-low pressure, hp-high pressure, cc-compression chamber, c-chamber, rc-resonating chamber, t-tube and vo-valve orifice)

Numerical results of some illustrative cases shown in Figure 6 are presented in Table 5. Different configurations, working fluids, capacities and pressure ranges have been worked out to show the versatility of the new program.

Table 5: Results for different compressor configurations

Case	Refrigerant	Capacity(cm^3)	P_{low} (bars)	P_{high} (bars)	\dot{m} (kg/hr)	T_{in} ($^{\circ}C$)	T_{out} ($^{\circ}C$)	W (J)
a ₁	R134a	8.095	2	14	10.56	32	108.74	-3.61
a ₂	R134a	8.095	1.14	14	5.38	32	125.84	-2.39
b	R600a	15.97	1.08	7.72	6.37	32	108.60	-4.78
c	R744	1.29, 0.95	30	80	15.17	32	99.04	-4.63

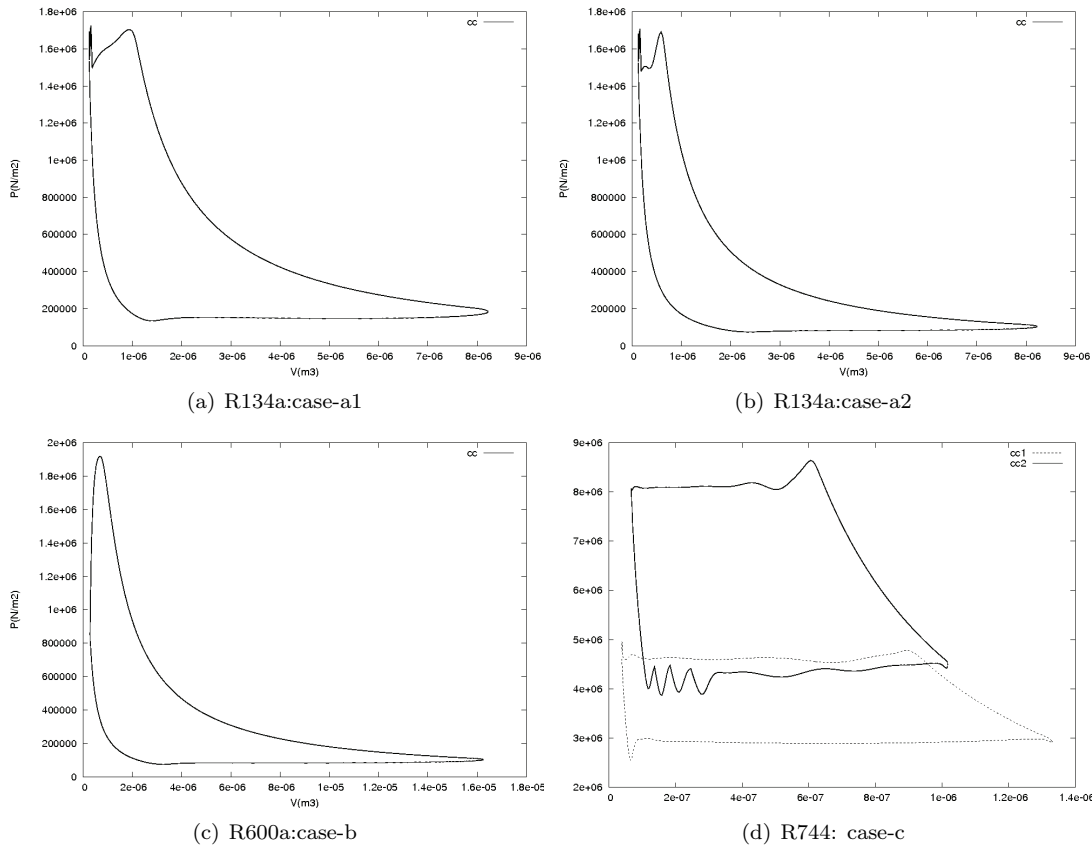


Figure 7: P-V diagrams of some of the illustrative cases

8. CONCLUSION

A new object oriented program for the numerical simulation of the thermal and fluid dynamic behaviour of hermetic reciprocating compressors has been developed. The object oriented approach offers the use of multiple paths, several compression chambers in parallel or in series etc., and adapts faster to different compressor configurations by adding/removing the required elements. Finally, numerical results of some illustrative cases are presented to show the advantages offered by the new program.

REFERENCES

1. Pérez-Segarra, C.D., Escanes, F., Oliva, A., 1994, Numerical Study of the Thermal and Fluid-Dynamic Behaviour of Reciprocating Compressors, *International Compressor Engineering Conference*, Purdue University, West Lafayette, Indiana, USA, p. 145-150.
2. Escanes, F., Pérez-Segarra, C.D., Rigola, J., Serra, J.M., 1996, Numerical Simulation of Reciprocating

- Compressors. Recent Improvements and Experimental Validation, *International Compressor Engineering Conference*, Purdue University, West Lafayette, Indiana, USA, p. 193-198.
3. Rigola, J., Pérez-Segarra, C.D., Oliva, A., Serra, J.M., Escribà, M., Pons, J., 1998, Parametric Study and Experimental Validation of Small Hermetic Refrigeration Compressors Using a Complete Advanced Numerical Simulation Model, *International Compressor Engineering Conference*, Purdue University, Indiana, USA, Vol. I, p. 737-742.
 4. Pérez-Segarra C.D., Rigola, J., Oliva, A., 2003, Modelling and numerical simulation of the thermal and fluid dynamic behaviour of hermetic reciprocating compressors. Part 1. Theoretical basis, *Int J Heating, Ventilating, Air-Conditioning Refrigerating Res* 9, p. 215-236.
 5. Rigola, J., Pérez-Segarra, C.D., Oliva, A., 2003, Modelling and numerical simulation of the thermal and fluid dynamic behaviour of hermetic reciprocating compressors. Part 2. Experimental investigation, *Int J Heating, Ventilating, Air-Conditioning Refrigerating Res* 9, p. 237-249.
 6. Rigola, J., Raush, G., Pérez-Segarra, C.D., Oliva, A., 2004, Detailed Experimental Validation of the Thermal and Fluid Dynamic Behaviour of Hermetic Reciprocating Compressors, *Int J Heating, Ventilating, Air-Conditioning Refrigerating Res* 10, p. 291-306.
 7. Patankar, S.V., 1980, *Numerical Heat Transfer*, Hemisphere publishing corporation.
 8. Morse, P.M., Feshbach, H., 1953, *Methods of Theoretical Physics, part 2*, McGraw-Hill Book Company.
 9. Browler, W.B., Eisler, Jr.E., Gonenc, E.J., Plati, C., Stagnitti, J., 1993, On the compressible flow through an orifice, *J. Fluid Engineering*, 115, p. 660-664.

NOMENCLATURE

Latin symbols

p	pressure(N/m ²)	p'	pressure correction
h	enthalpy(J/kg)	m	mass(kg)
t	time(sec)	\dot{m}	mass flow rate(kg/sec)
CV	control volume	W	work(J)
v	velocity(m/s)	l	constriction length(m)
e_c	kinetic energy(J)	V	Volume(m ³)
\dot{Q}	heat rate(J/sec)	N	area(m ²)
S^I, S^{II}	areas(m ²) of cross-sections i and o	M, H	terms from momentum equation of tubes and valve orifices
S^S	$\min(S^I, S^{II})$	c_c	expansion/contraction coefficient
<i>Greek symbols</i>			
ϕ	generic variable(p, h, v)	ρ	density(kg/m ³)
ϵ	precision demanded	ρ'	density correction
Π	compressible flow parameter	γ	ratio of specific heats of a gas
α	relaxation factor for p'		
<i>Superscripts</i>			
*	guess value	**	value at previous iteration
0	value at previous time step		
<i>Subscripts</i>			
P	central point or CV under consideration	W	point or CV to left(west) of P
E	point or CV to right(east) of P	k	connection index to the chamber
(-)-overbar	integral mass averages over CV	(~)tilde	integral volume average over CV
w	control volume face between W and P	e	control volume face between P and E

ACKNOWLEDGEMENTS

The authors gratefully acknowledge the financial support provided by ACC Compressors Spain, S.A. - Unidad Hermética division (ref. no. C06244).